PCCP

Accepted Manuscript

This is an *Accepted Manuscript*, which has been through the Royal Society of Chemistry peer review process and has been accepted for publication.

Accepted Manuscripts are published online shortly after acceptance, before technical editing, formatting and proof reading. Using this free service, authors can make their results available to the community, in citable form, before we publish the edited article. We will replace this *Accepted Manuscript* with the edited and formatted *Advance Article* as soon as it is available.

You can find more information about *Accepted Manuscripts* in the Information for Authors.

Please note that technical editing may introduce minor changes to the text and/or graphics, which may alter content. The journal's standard Terms & Conditions and the Ethical guidelines still apply. In no event shall the Royal Society of Chemistry be held responsible for any errors or omissions in this *Accepted Manuscript* or any consequences arising from the use of any information it contains.

ROYAL SOCIETY OF CHEMISTRY

www.rsc.org/pccp

Cite this: DOI: 10.1039/c0xx00000x

www.rsc.org/xxxxxx

ARTICLE TYPE

pH Assisted control over binding and relocation of acridine guest between a macrocyclic nanocarrier and natural DNA †

Mhejabeen Sayed[a,*] and Haridas Pal[a,*]

Received (in XXX, XXX) Xth XXXXXXXXX 20XX, Accepted Xth XXXXXXXXX 20XX

DOI: 10.1039/b000000x

Differential binding affinity of hydroxypropyl-β-cyclodextrin (HPβCD) macrocycle, a drug delivery vehicle, towards protonated and deprotonated forms of the well-known DNA binder and a model anticancer drug, acridine, has been exploited as a strategy for dye/drug transportation and pH responsive delivery to natural DNA target. From pH sensitive changes in the ground state absorption and steady-state fluorescence characteristics of the studied acridine dye/HPβCD/DNA ternary system and strongly supported by fluorescence lifetime, fluorescence anisotropy, Job's plots, ^{1}H NMR and circular dichroism results it is revealed that in a moderately alkaline solution (pH ~8.5), the dye can be predominantly bound to HPβCD macrocycle and when pH is lowered to a moderately acidic region (pH ~4), the dye efficiently detaches from HPβCD cavity and almost exclusively binds to DNA. In the present study we are thus able to construct a pH sensitive supramolecular assembly where pH acts as a simple stimulus for controlled uptake and targeted release of the dye/drug. As pH is an essential and sensitive factor in various biological processes, such a simple yet reliable pH sensitive model demonstrated here can have promising applications in host-assisted delivery of prodrug at the target sites, such as cancer or tumour microenvironments, with an enhanced stability, bioavailability and activity, and also in the design of new fluorescent probes, sensors and smart materials for applications in nano-sciences.

Introduction

Supramolecular assemblies formed involving non-covalent interactions have currently attracted immense research interests due to their diverse utility in areas like drug delivery,[1, 2] nanotechnology,[3] food industry,[4] on–off switches,[5] catalysis,[6] photostabilization,[2, 7] photodynamic therapy,[8] optical sensors,[9] and many others.[10, 11] The underlying non-covalent host-guest interactions have great potentials for developing excellent tunable functional materials because of their strong responses to external stimuli like pH,[1, 12-15] salt,[11, 15] temperature,[5, 15] light,[5] etc. Stimuli responsive targeted drug delivery, particularly involving macrocyclic hosts as carriers, are currently undergoing great advances where pH, salt or light can act as a trigger for controlled cargo drug release at the target site for its desired effects with enhanced efficiency.[2, 5, 11-15] In supramolecular drug delivery applications, the drug carrier vehicle plays a vital role to transport the drug specifically at the required location and thus increasing the concentration and also the effectiveness of the drug at the targeted site, which in turn reduces the toxicity and the undesired side effects to the normal cells.[1, 2, 13-16] Cyclodextrins (CD) as macrocyclic hosts have been very successfully used as drug carriers in many drug formulations.[1, 16, 17]

CDs are unique cyclic polysaccharides formed by D-glucopyranose monomer units joined by ether linkages in a cyclic manner and thus provide hydrophobic cavities where nonpolar/hydrophobic residues of the guest molecules can be encapsulated to form inclusion complexes via non-covalent interactions.[7, 13, 18-21] Depending upon the number of D-glucopyranose units present, different CD homologues with varying cavity sizes exists, namely αCD, βCD and γCD, containing 6, 7, and 8 monomer units, respectively. Cyclodextrins and their derivatives show low toxicity, high biocompatibility, excellent inclusion capability with variety of drug/dye molecules, which make them attractive for uses in several drug formulations and many biomedical applications.[1, 2, 7, 8, 13-17] In this regard CD derivatives with polar substituents are more promising than the parent CD hosts. For example, hydroxypropyl-β–cyclodextrin (HPβCD; Scheme 1), show dramatically increased water solubility and much enhanced binding interactions in comparison to parent CDs and thus can largely improve the bioavailability of the drugs. Moreover, like CDs, the HPCDs have also been reported to be well tolerated in humans.[1, 22] Recently, Huang et al. have reported significantly improved water solubility, thermal stability, dissolution rate and increased sprout inhibition effect of potato for the drug chlorpropham on complexation with HPβCD.[23] Miyake, et al. have also reported that the drug rutin shows increased bioavailability in a formulation made with HPβCD compared to βCD.[24]

DNA is considered to be one of the primary intracellular target for anticancer drugs, where the drug can cause the selective damage of the cancer cell,[25-27] taking advantage of the acidic pH condition of the cancerous organelles.[13, 28] Acridine dye and its derivatives are widely used in antitumor treatment as well as in

Physical Chemistry Chemical Physics Accepted Manuscript

chemotherapy. Many new acridine derivatives are being prepared to improve their DNA binding properties with superior antitumor activity.[26, 29-31] Selective delivery of such anticancer drugs at the target site having low pH like tumour cells may increase the localized cytotoxicity and lower the side effects of the drug towards healthy cells.

In the present study we have investigated the interaction of model anticancer drug acridine, with HPβCD and a biomolecular target DNA at different pH conditions in aqueous solution, to realize if a pH responsive release of the model drug to the target can be achieved. Acridine is a prototropic dye (cf. Scheme 1), with its pK_a as 5.4.[19] Thus, in aqueous solution it exists in the protonated form (AcH^+) at acidic pH and in neutral form (Ac) at alkaline pH.[19] Acridine and its derivatives are potent DNA binder because of their planar structures,[29, 30, 32] and are well recognized as drugs showing carcinogenic effect due to their property to bind strongly with DNA. Acridine dyes are reported to exhibit two modes of binding with DNA: intercalative binding where planar ring of acridines intercalate into the DNA base pairs, and semi-intercalative or exo-binding where electrostatic interaction of phosphate back bone of DNA plays the major role.[33-35] Significant microenvironment sensitive changes in the spectroscopic properties of acridine dyes make them useful fluorescence probes to study local environments in various microheterogeneous systems.[36-38] Taking advantage of the strikingly different binding behaviour of HPβCD macrocycle towards protonated and neutral forms of acridine dye, as observed in the present study, we have demonstrated an effective pH triggered controlled and targeted release of the dye from HPβCD cavity, a potential drug carrier vehicle, to the target site of DNA, which is a major goal in chemotherapeutic applications. Though in the literature, interaction of organic dyes with cyclodextrins and DNA has been reported[39, 40] but detailed pH responsive investigations on such supramolecular assemblies are very limited. In contrast to involved multi-step synthesis and sophisticated detection methods, we present here a simple yet reliable pH responsive model study using photochemical measurements, which can open up new opportunities in engineering intelligent functional materials useful for various biomedical applications.

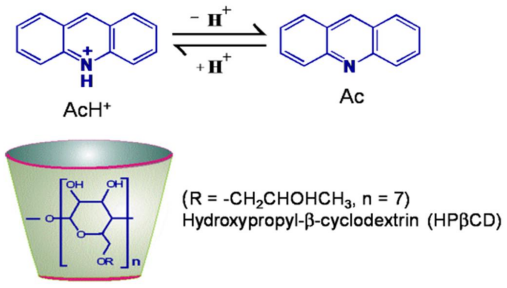

Scheme 1: Prototropic equilibrium of acridine dye and HPβCD host used in this study are shown for quick visualization.

Results and Discussion

1.1. Interaction of acridine dye with DNA and HPβCD hosts

1.1.1. Ground state absorption and steady-state fluorescence studies: The ground-state pK_a of acridine dye is 5.4 and both protonated (AcH^+) and neutral (Ac) forms of the dye exhibit prominent absorption and fluorescence spectral features in the solution at suitable pH conditions.[19] In the steady-state (SS) fluorescence studies, both AcH^+ and Ac forms of the dye are clearly distinguished at pH 4 and 8.5 from their characteristic fluorescence maxima at 482 nm and 430 nm, respectively. Upon addition of DNA to either of these solutions (at pH 4 and 8.5, respectively), there is a gradual decrease in the fluorescence intensity, as are shown in Figure 1a & b for the respective cases. These results clearly indicate a strong interaction for both the prototropic forms of the dye with DNA. Changes in the fluorescence intensity (ΔI_f) with DNA concentration were correlated following eq. 1 (cf. Note 1, SI) to evaluate the binding constant (K_{eq}) for both the forms of the dye.

$$\Delta I_f = \Delta I_f^{\infty} \frac{K_{eq}[B]^n}{1 + K_{eq}[B]^n} \qquad (1)$$

where, ΔI_f^{∞} is the final change in the fluorescence intensity on complete complexation, $[B]$ represents the DNA concentration in terms of total nucleotides and n is the number of nucleotides involved per molecule of the dye binding. Analyses of the fluorescence data following eq. 1 and considering ΔI_f^{∞} and K_{eq} as the fitting parameters provide the best fits to the data when n is assumed to be 2 (cf. Insets in Figure 1a & b). The K_{eq} values thus obtained for AcH^+/DNA and Ac/DNA systems are 1.9×10^7 M^{-2} and 3.1×10^7 M^{-2}, respectively. The magnitudes of these K_{eq} values are very high and thus suggest extremely strong binding for both the forms of the dye with DNA. Due to such strong binding with DNA, acridine dye is employed as a useful biological probe and also as a photoactivator towards DNA. It should be noted that similar high binding affinity have also been reported in the literature for other typical intercalator dyes with DNA.[41] About 1.6 times higher binding constant for Ac/DNA complex compared to AcH^+/DNA complex indicates that the neutral form of the dye undergoes a relatively stronger binding with DNA than its protonated form. The result suggests that due to the neutral nature, the Ac undergoes stronger intercalative mode of binding with DNA, through hydrophobic interaction, compared to AcH^+, for which electrostatic interaction would be the most likely binding mode.

Ground state absorption behaviour was also examined for both AcH^+ and Ac forms of the dye in the presence of DNA. Absorption maximum for both the forms of the dye appears at about 354 nm. The AcH^+ form is, however, distinctly characterized by its broad longer wavelength shoulder absorption band spreading in the 380-440 nm region, which is absent for the neutral form of the dye.[19] Upon gradual addition of DNA to AcH^+ and Ac solutions (at pH 4 and 8.5, respectively), the peak absorbance show a gradual decrease along with small bathochromic shifts (~1 nm for AcH^+ and ~3 nm for Ac for the 354 nm band) and the appearance of isosbestic point like features at ~360 nm for AcH^+ and ~392 nm for Ac (cf. Figure S1 in the supporting information, SI). These results are thus in corroboration with the SS fluorescence results presented in Figure 1a and b suggesting a strong binding interaction for both the prototropic forms of the dye with DNA host.

The n value of 2 obtained from the analysis of the fluorescence titration data for both AcH^+/DNA and Ac/DNA systems indicates

This journal is © The Royal Society of Chemistry [year]

Physical Chemistry Chemical Physics Accepted Manuscript

that there are simultaneous involvement two nucleotides in the binding of a dye molecule to the DNA host. To verify such a stoichiometry further for the host-guest complexes in the AcH^+/DNA and Ac/DNA systems, we carried out the Job's plot measurements[42, 43] following both absorption and fluorescence studies. Figure 2a and b show the Job's plots for the AcH^+/DNA (pH 4) and Ac/DNA (pH 8.5) systems, respectively, obtained from fluorescence measurements. The Job's plots for these systems as obtained from absorption measurements are shown in Figures S2 in the SI. The maxima of these Job's plots appear at around 0.33 mole fraction of the dye and thus unambiguously establishing the 1:2 (dye to host) stoichiometry of the complexes formed both in AcH^+/DNA and Ac/DNA systems.

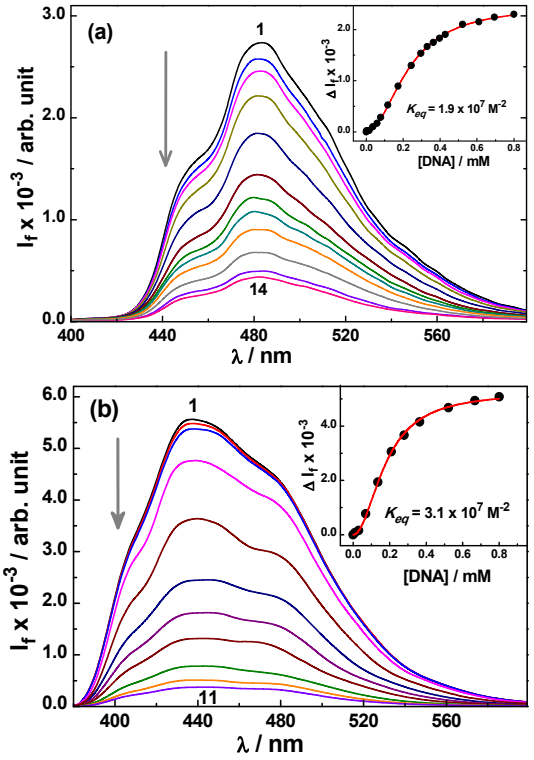

Figure 1. (a) Changes in the SS fluorescence spectra for AcH^+/DNA system at pH 4; [AcH^+] = 10.2 μM and [DNA] = 0, 36, 59, 78, 117, 172, 244, 296, 330, 396, 429, 522, 694 and 800 μM for spectra 1–14. **Inset:** Fluorescence titration curve for AcH^+/DNA system at pH 4, analysed using eq. 1 with n = 2. **(b)** Changes in the steady-state fluorescence spectra for Ac/DNA system at pH 8.5; [Ac] = 10.5 μM and [DNA] = 0, 10, 30, 69, 135, 209, 279, 364, 522, 667 and 800 μM for spectra 1–11. **Inset:** Fluorescence titration curve for Ac/DNA system at pH 8.5, analysed using eq. 1 with $n = 2$.

Knowing the strong interaction of the dye with DNA, we subsequently carried out absorption and SS fluorescence measurements to explore the interaction of the dye with the recognized drug carrier, HPβCD. For the Ac form of the dye (pH 8.5), with an increase in the HPβCD concentration, there is a gradual decrease in the fluorescence intensity, along with the concomitant development of two new vibrational features in the spectra at ~427 and 445 nm and also a small hypsochromic shift in the emission maxima, as shown in Figure 3. These results indicate quite strong inclusion complex formation for the Ac form of the dye with HPβCD host. The hypsochromic shift and the development of vibrational features clearly suggest that the bound dye experiences a relatively lower micropolarity on incorporation into the HPβCD cavity than in the bulk water. Reduction in the fluorescence intensity for the Ac/HPβCD systems is justifiably assigned to the strong hydrogen bonding interaction of the encapsulated Ac with the portal OH groups of the HPβCD host, as also observed in our earlier study on the interaction of the dye with the unsubstituted βCD host.[19]

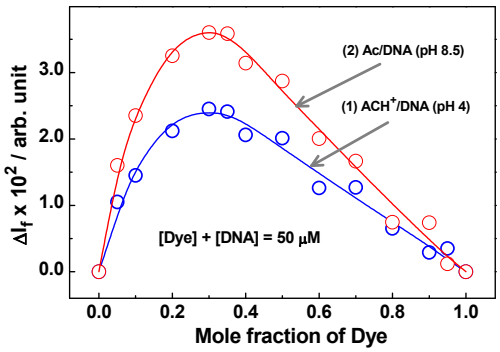

Figure 2: Job's plots for AcH^+/DNA (pH 4) and Ac/DNA (pH 8.5) systems obtained from fluorescence changes ($\Delta I_f = I_{Dye/Host} - I_{dye\text{-}only}$) as a function of the constituents. The sum of the dye and the host concentrations in these measurements was kept constant at 50 μM. Excitation and emission wavelengths were 360 nm and 482 nm for AcH^+/DNA and 361 nm and 430 nm for Ac/DNA system.

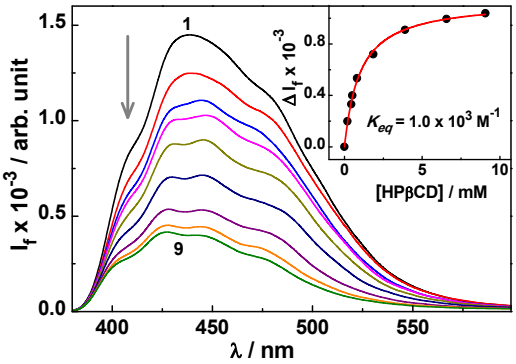

Figure 3: Changes in the SS fluorescence spectra for Ac/HPβCD system at pH 8.5; [Ac] = 13.6 μM and [HPβCD] = 0, 0.2, 0.43, 0.5, 0.81, 1.85, 3.9, 6.6, and 9.1 mM for spectra 1–9. **Inset:** Fluorescence titration curve for Ac/HPβCD system at pH 8.5, analysed using eq. 1 with n = 1.

In accordance with the SS fluorescence results, in the absorption studies also there is a small decrease in the absorbance along with a small red shift (~ 2nm) in the absorption maximum for the Ac form (pH 8.5) of the dye on addition of the HPβCD host in the solution (cf. Figure S3a, SI). Observed results support a reasonable host-guest interaction in the Ac/HPβCD system. Unlike the neutral Ac form, the protonated AcH^+ form of the dye, however, did not show any appreciable change, either in the absorption (cf. Figure S3b, SI) or in the fluorescence (cf. Figure S4, SI) characteristics, on addition of the HPβCD host in the solution. These observations suggest that the interaction of the AcH^+ form of the dye with HPβCD host is extremely weak in comparison to that of the neutral Ac form of the dye.

Job's plot study[42, 43] was carried out for Ac/HPβCD system at pH 8.5 to explore the stoichiometry of the complex formed in this case. Due to very small changes that occur in the absorbance of Ac on addition of HPβCD host (cf. Figure S3a SI), no meaningful

Physical Chemistry Chemical Physics Accepted Manuscript

Job's plot could be obtained for Ac/HPβCD system from absorption measurement. Satisfactory Job's plot for the present system, however, could be obtained from fluorescence study, as shown in Figure 4, indicating the maximum at around 0.5 mole fraction of the dye and thus suggesting the 1:1 stoichiometry of complex formed in this system. For the AcH^+/HPβCD (pH 4) system, as the interaction was found to be extremely weak from both absorption and fluorescence studies (cf. Figures S3b and S4, SI), Job's plot measurement was not attempted for this system.

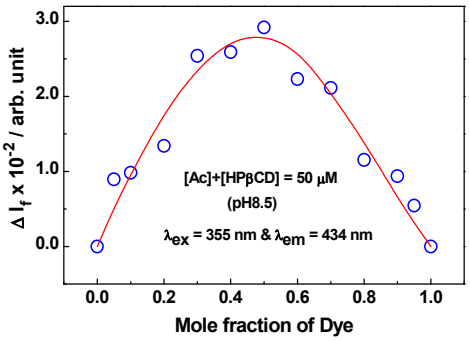

Figure 4: Job's plot obtained for Ac/HPβCD (pH 8.5) system using fluorescence measurement. The sum of the dye and the host concentrations in these measurements was kept constant at 50 μM. Excitation and emission wavelengths were 354 nm and, respectively.

Fluorescence titration method was utilized to evaluate the binding constant (K_{eq}) value for the Ac/HPβCD system. As shown in the Inset of Figure 3, the changes in the fluorescence intensity (ΔI_f) as a function of the host concentration fit well with the consideration of 1:1 complex formation (cf. eq. 1 with n =1), as suggested from Job's plot. The K_{eq} value thus estimated for the Ac/HPβCD complex is about 1.0×10^3 M^{-1}. It should be mentioned here that the binding interaction of Ac with HPβCD is about 3.4 times higher than that observed with parent βCD host, reported in our earlier study.[19] It is thus evident that the extended cage structure offered by HPβCD host renders a much greater hydrophobic interaction for the Ac form of the dye, leading to a stronger inclusion complex formation. For the AcH^+ form of the dye, as there was no appreciable change either in the absorption or in fluorescence characteristics (cf. Figures S3b and S4, SI), no titration study could be carried out for AcH^+/HPβCD system to estimate the binding constant value.

1.1.2. ^{1}H NMR studies on the dye-host systems: To get an insight of the mode of binding in the present dye-host systems, the ^{1}H NMR measurements were carried out in D_2O solution. Figure 5 shows the NMR spectra obtained for free Ac and Ac-HPβCD systems recorded at pD 8.5. As indicated from this figure, the NMR signals for all the aromatic protons of Ac undergo small downfield shift on interaction with HPβCD. Since both the ends of Ac along its long axis are equivalent, an axial incorporation of the dye into the HPβCD cavity can involve either of its axial ends equally. Therefore, the NMR signals for all the aromatic protons of Ac are expected to undergo very similar shifts, as we observe experimentally. To be mentioned here that similar downfield shifts in the NMR signals for all the aromatic protons of Ac have also been reported in the literature for its interaction with parent βCD host.[44] One interesting observation in the present NMR results for the Ac-HPβCD system is that the two NMR peaks at the middle of the apparent quartet associated with the H1 and H4 protons of Ac almost get merged to each other on interaction of the dye with HPβCD host, a unique feature not observed earlier for the Ac-βCD system.[44] This is certainly due to different extent of shifts for the H1 and H4 proton signals on interaction of the dye with HPβCD, though exact details of these shifts could not be unraveled from the present study. For the AcH^+-HPβCD system (pH 4), since no appreciable dye-host interaction was indicated from absorption and fluorescence measurements (cf. Figures S3a and S4, SI), no NMR study was attempted for this system.

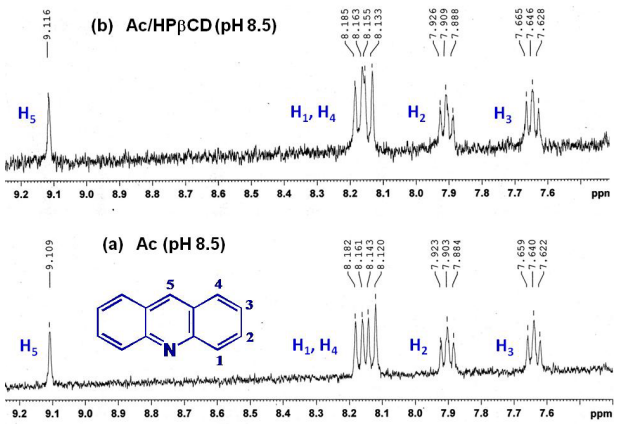

Figure 5: 1H NMR spectra of (a) free Ac and (b) Ac-HPβCD systems obtained at pH 8.5. Concentrations of the components were: [Ac] = 150 μM and [HPβCD] = 150 mM.

The ^{1}H NMR studies were also carried out for the Ac-DNA system in D_2O solution at pD 8.5. The NMR spectra recorded for the free Ac and Ac-DNA system under similar experimental conditions are shown in Figure S5 of SI. As indicated from this figure, there are no distinguishable NMR signals for the Ac-DNA system that can be attributed either to the guest dye or to the DNA host (cf. Figure S5b of SI), even though characteristic NMR signals are clearly observed for free dye in the absence of DNA under the similar experimental condition (cf. Figure S5a, SI). As the DNA molecules possess large number of exchangeable protons, it appears that in the present experimental conditions all the proton signals of DNA are broadened exceedingly largely causing the development of large background such that not only the DNA signals but also those of the guest dye get masked under this background. As the NMR results for the Ac-DNA system was not conclusive, a similar NMR study for the AcH^+-DNA system was not carried out in the present work.

1.1.3. Modulation in the prototropic equilibrium of the dye: Observing that the Ac and AcH^+ forms of the dye interact quite differently with both DNA and HPβCD hosts, it was expected that the dye will display significant modulation in its acid-base property on interaction with these hosts. Prototropic equilibrium for the dye in the presence of DNA or HPβCD hosts can be represented by a four-state dynamic equilibrium model as shown in Scheme 2, where K_a and K_a' represent the acid dissociation constants for the free and the bound dye and K_{eq} and K_{eq}' represent the binding constants for the Ac and AcH^+ forms of the dye with the host (H) used.

This journal is © The Royal Society of Chemistry [year]

Physical Chemistry Chemical Physics Accepted Manuscript

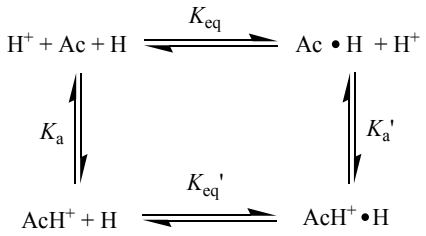

Scheme 2. Four-state thermodynamic equilibrium model for the acridine dye and host (H, either HPβCD or DNA) systems considering all the stages of host-guest interaction and the acid dissociation processes.

Modulations in the acid-base properties of the dye on its interaction with DNA and HPβCD hosts were investigated systematically following the pH dependent changes in the absorption spectra of the dye in the presence of significantly high concentrations of the hosts, as shown in Figure S6 of SI. Absorbance changes were noted at selected wavelengths in the absence as well as in the presence of DNA and HPβCD hosts, separately, as a function of pH of the solution, as are shown in Figure 6. The pK_a values were estimated from the inflection points of the plots and are found to be 5.4, 5.0 and 4.4 for the free dye, dye/DNA and Dye/HPβCD systems, respectively.

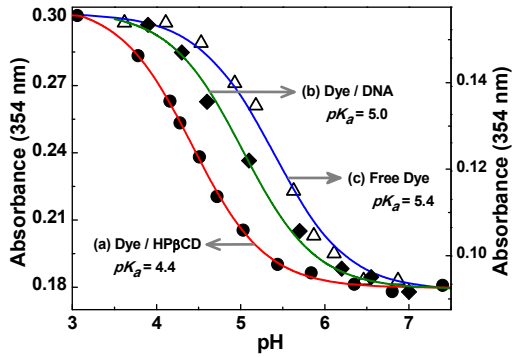

Figure 6: Changes in the absorbance of acridine dye (10 μM) at 354 nm measured in presence of (a) 30 mM HPβCD and (b) 800 μM DNA and (c) in the absence of any host, as a function of pH of the solution.

As indicated from the observed results, the pK_a value of the dye undergoes about 0.4 and 1.0 units of downward shifts, respectively, on its interaction with DNA and HPβCD hosts, which support the preferential binding of Ac form of the dye with both DNA and HPβCD hosts compared to the AcH^+ form, as inferred earlier from the fluorescence titration studies (cf. Section 1.1.1). The larger pK_a shift for the dye-HPβCD system (1.0 unit) compared to that of the dye-DNA system (0.4 unit) is directly in accordance with the observation that there is a larger difference in the binding affinities for the Ac and AcH^+ forms of the dye with HPβCD host than with DNA. Importantly, the difference in the pK_a shifts between the dye-DNA and dye-HPβCD systems can be exploited suitably to achieve a preferential binding for the dye, either to the DNA or to the HPβCD host, in a given dye/DNA/HPβCD ternary system, just by adjusting the pH of the solution, as are discussed in the following sections.

1.2. Competitive interaction of acridine dye with HPβCD and DNA hosts at pH 5.5: Competitive binding interaction of the two prototropic forms of acridine dye has been investigated at pH 5.5, a characteristic pH of cancer cells, in the simultaneous presence of both DNA and HPβCD hosts. As expected, at this pH, the absorption spectrum of the free dye (cf. Figure 7) exhibits a broad absorption shoulder at the longer wavelength region (~400-440), an exclusive feature for the AcH^+ form of the dye, along with the absorption maximum at 354 nm. These observations are consistent with the pK_a value of 5.4 of the dye,[19] suggesting the presence of both AcH^+ and Ac forms of the dye in the solution at pH 5.5, both with significant proportions (almost 50:50).

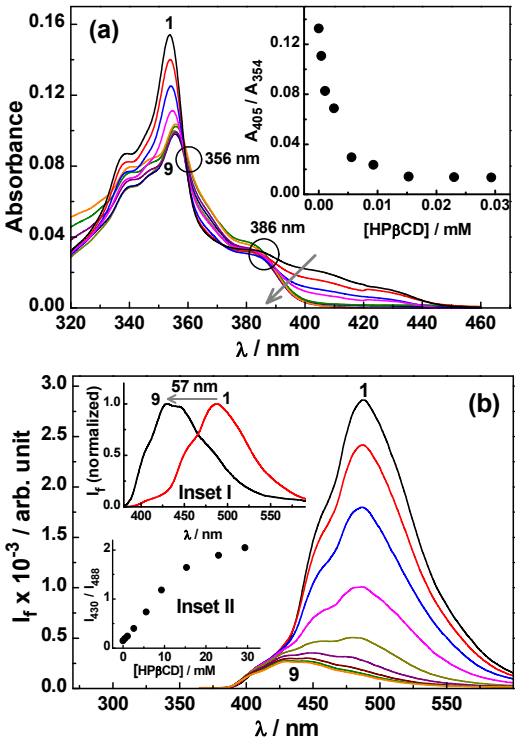

Figure 7. (a) Changes in the absorption spectra for Ac/HPβCD system at pH 5.5; [Ac] = 10 μM and [HPβCD] = 0, 0.46, 1.08, 2.6, 5.6, 9.3, 15.3, 23, and 29.4 mM for spectra 1–9. **Inset:** Ratio of absorbance at 405 and 354 nm (A_{405}/A_{354}) as a function of HPβCD concentration. **(b)** Changes in the SS fluorescence spectra for Ac/HPβCD system at pH 5.5; [Ac] = 10.6 μM and [HPβCD] = 0, 0.46, 1.08, 2.6, 5.6, 9.3, 15.3, 23, and 29.4 mM for spectra 1–9. **Inset I**: Normalized fluorescence spectra for (1) only Ac and (9) Ac/HPβCD (29.4 mM) at pH 5.5. **Inset II**: Ratio of fluorescence intensity ratio at 430 and 488 nm (I_{430}/I_{488}) as a function of HPβCD concentration.

Figure 7a, shows the changes in the absorption spectra of the dye with the changing HPβCD concentration at pH 5.5. With an increase in HPβCD concentration, there is a decrease in the absorbance for both the 354 nm main band and the 400-440 nm shoulder band along with a small red shift of the main absorption band by ~3 nm. These changes are certainly due to the dye/HPβCD inclusion complex formation. Interestingly, it is observed from Figure 7a that in the presence of HPβCD at pH 5.5, there is a relatively larger decrease in the absorbance for the 400-440 nm shoulder band in comparison to that of the 354 nm main band. This observation suggests that the relative proportion of the Ac form enhances in the solution on increasing the HPβCD concentration, as a consequence of the downward pK_a shift of the dye due to preferential Ac/HPβCD complex formation. Appearance of the kind of isosbestic points at about 360 and 386 nm in the absorption spectra with the increasing HPβCD

Physical Chemistry Chemical Physics Accepted Manuscript

concentration also supports the conversion of some of the AcH^+ to Ac form through the preferential formation of the Ac/HPβCD complex. This is further indicated by the plot shown in the Inset of Figure 7a, displaying a sharp decrease in the ratio of absorbance at 405 nm (mainly due to AcH^+) to 354 nm (both AcH^+ and Ac contributes) with an increase in the HPβCD concentration.

Studies on acridine dye/HPβCD system at pH 5.5 have also been carried out using SS fluorescence measurements and the results are shown in Figure 7b. It is observed that on increasing HPβCD concentration there is a large decrease in the fluorescence intensity along with a large blue shift in the emission peak, as large as ~57 nm (cf. Inset I of Figure 7b). These results clearly manifest the switch over of the large fraction of the AcH^+ emission in the absence of HPβCD to the predominantly Ac emission in the presence of HPβCD, suggesting the host-assisted deprotonation of AcH^+ at the studied pH condition. It is thus evident that, without changing the pH, one can change the proportions of the prototropic forms of the dye in the solution, just by the addition of the HPβCD host. Inset II of Figure 7b, shows the plot of fluorescence intensity ratio (I_{430}/I_{488}) for the dye at 430 nm (Ac) to 488 nm (AcH^+), as a function of the increasing HPβCD concentration. As revealed form this plot, the intensity ratio increases sharply on increasing the host concentration, indicating the preferential Ac/HPβCD inclusion complex formation in the system and thereby shifting the overall prototropic equilibrium of the dye gradually towards the Ac form. The K_{eq} value for the Ac-HPβCD system was also estimated from fluorescence titration data at pH 5.5 (cf. Figure S7a, SI) and is found to be 560 M^{-1}, two times lower than the value estimated at pH 8.5. This reduction in the K_{eq} value arises because at pH 5.5 a fraction of dye remains in the protonated form which does not interact with HPβCD (cf. Section 1.1.1).

As discussed in section 1.1, both HPβCD and DNA show largely different binding affinities for AcH^+ and Ac forms of the dye. Such a property can be exploited to control the binding of the dye preferentially to either HPβCD or DNA hosts, simply by adjusting the pH of the solution. To realize such a control and to apprehend a possible dye relocalization from HPβCD to DNA, the photochemical changes for the dye (10uM)/HPβCD (30mM) system at pH 5.5 was further explored in the presence of varying DNA concentrations. Figure 8a depicts the changes in the absorption spectra of Ac/HPβCD system with the changing DNA concentration. The results show an appreciable regain of the broad longer wavelength shoulder band, of the AcH^+ form of the dye, implying that the dye slowly detaches from the Ac/HPβCD complex and subsequently binds to the DNA host through protonation of the detached dye. This is further evidenced from the appearance of the clear isosbestic point at ~390 nm. Formation of good extent of AcH^+/DNA complex is also supported by the comparison of the absorption spectra in the related binary and ternary systems (cf. Inset I of Figure 8a) and by the changes in the absorbance ratio for 415 nm to 356 nm for the ternary system (cf. Inset II of Figure 8a). Observed results clearly indicate that at pH 5.5, the dye prefers to bind to DNA host over HPβCD, through the formation of the AcH^+/DNA complex in lieu of the Ac/HPβCD complex. This is in accordance with the higher pK_a value (5.0) for the dye/DNA system as compared to that (4.4) of the dye/HPβCD system.

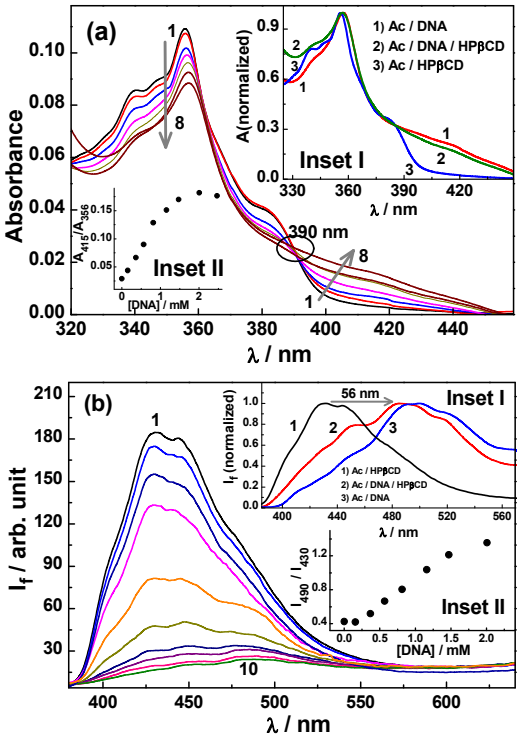

Figure 8. (a) Changes in the absorption spectra for Ac/HPβCD system upon addition of DNA at pH 5.5; [Ac] = 11 μM, [HPβCD] = 30 mM and [DNA] = 0, 0.156, 0.369, 0.569, 0.814, 1.160, 2.015, and 2.47 mM for spectra 1–8. **Inset I:** Normalized absorption spectra for (1) Ac/DNA, (2) Ac/DNA/HPβCD, (3) Ac/HPβCD at pH 5.5; [Ac] = 11 μM, [HPβCD] = 30mM and [DNA] = 2.47 mM. **Inset II:** Ratio of absorbance at 415 and 355 nm with increasing DNA concentration. **(b)** Changes in the SS fluorescence spectra for Ac/HPβCD system upon addition of DNA at pH 5.5; [Ac] = 11 μM, [HPβCD] = 30mM and [DNA] = 0, 0.068, 0.156, 0.369, 0.569, 0.814, 1.160, 1.472, 2.015, and 2.47 mM for spectra 1–10. **Inset I**: Normalized fluorescence spectra for (1) Ac/HPβCD, (2) Ac/DNA/HPβCD, (3) Ac/DNA at pH 5.5. [Ac] = 11 μM, [HPβCD] = 30mM and DNA = 2.47 mM. **Inset II**: Ratio of fluorescence intensity at 490 and 430 nm with increasing DNA concentration.

The fluorescence spectral features of Ac/HPβCD system at pH 5.5 also undergo large changes on the addition of DNA, as shown in Figure 8b. With an increase in the DNA concentration, fluorescence intensity undergoes a large reduction, indicating the disruption of dye/HPβCD complex in the presence of DNA. Additionally, the fluorescence peak at 430 nm slowly disappears and a prominent new peak appears at 487 nm, illustrating the substantial formation of AcH^+/DNA complex in the system. In the present case, since the solution pH is close to the dye pK_a, a reasonable amount of Ac/HPβCD and Ac/DNA complexes are present in the solution, as indicated by the small hump at around 450 nm for Ac/DNA/HPβCD system (cf. Inset I of Figure 8b). Comparison of the fluorescence spectra for the relevant binary and ternary systems, as shown in the Inset I of Figure 8b, it is clearly exemplified that DNA dominates the binding of the dye at pH 5.5 as compared to HPβCD host. It is noticed from Inset II of Figure 8b that the fluorescence intensity ratio for acridine dye at 490 to 430 nm (I_{490}/I_{430}) increases reasonably sharply with an increase in the DNA concentration. This observation is directly in corroboration with the fact that at pH 5.5 the dye shows a preferential binding towards DNA than HPβCD, resulting a major fraction of the dye to undergo relocation from HPβCD nanocavity

This journal is © The Royal Society of Chemistry [year]

Physical Chemistry Chemical Physics Accepted Manuscript

to DNA pocket. Thus, at pH 5.5, the HPβCD in effect plays the role of a drug transport vehicle, supplying the dye/drug for binding to DNA target. Binding constant value for the formation of the new AcH^+/DNA complex in the presence of HPβCD was estimated following equation 1 and is found to be $4.6x10^6$ M^{-2}, which is ~4 times lower than the value estimated at pH 4 in the absence of HPβCD (Figure S7b, SI). This is expected because there is a competition between DNA and HPβCD to bind the dye and hence the dye binding with DNA is significantly affected by the presence of HPβCD and vice versa. In the present case also, the number of nucleotides (n) required to bind a dye is found to be two (cf. Figure S7b, SI), similar to that obtained in the absence of HPβCD host at pH 4 and 8.5, suggesting that the HPβCD does not have any direct interaction with DNA such that the mode of dye binding to DNA remains unaltered. It should be noted here that in the literature also it is well documented that there is hardly any interaction of cyclodextrin hosts with DNA.[45, 46]

1.3. pH triggered delivery of acridine dye from HPβCD host to DNA: As binding interactions in the studied systems are noncovalent in nature, it is interesting to see if the dye binding and relocation between HPβCD and DNA can be controlled at ones will by using pH as a stimulus, which can eventually be exploited rationally in applications like controlled drug delivery. Taking into consideration of the pH range where denaturation of DNA does not take place (pH 4 to 9),[47-50] we investigated systematically the dye/HPβCD/DNA ternary system at two different pH conditions, namely pH 4 and 8.5, where acridine dye will exist mainly in the AcH^+ and Ac forms, respectively. Results of these studies are very intriguing and are described in the following sections.

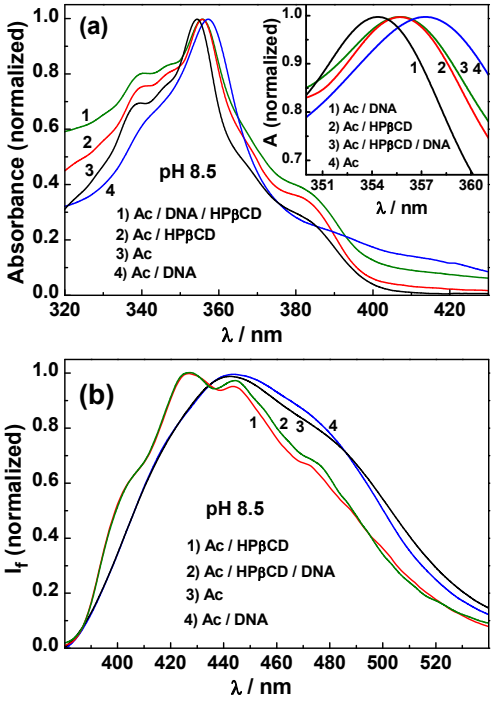

Figure 9. (a) Normalized absorption spectra for Ac/DNA/HPβCD, Ac/HPβCD, Ac and Ac/DNA systems at pH 8.5. [Ac] = 11 μM, [HPβCD] = 10 mM and DNA = 2.0 mM. **(b)** Normalized steady-state fluorescence spectra for Ac/HPβCD, Ac/HPβCD/DNA, Ac and Ac/DNA systems at pH 8.5. [Ac] = 11 μM, [HPβCD] = 10 mM and DNA = 2.0 mM.

1.3.1. Absorption and fluorescence studies: The absorption and fluorescence spectra of the dye in the dye/HPβCD/DNA ternary system at pH 8.5 are shown in Figure 9a and b and those at pH 4 are shown in Figure 10a and b, respectively. Absorption and fluorescence spectra for the dye in the dye/HPβCD, Dye/DNA and Dye alone cases at the respective pH conditions are also shown in the corresponding figures for comparison. As indicated from Figure 9a and b, at pH 8.5, the normalized absorption and fluorescence spectra of the dye/HPβCD/DNA ternary system resemble quiet closely to those of the dye/HPβCD system, with prominent absorption peak at 356 nm and dual emission peaks centred at 427 and 445 nm, indicating preferential binding of Ac to HPβCD in dye/HPβCD/DNA ternary system. For Ac-DNA binding at pH 8.5, considering n equal to two and assuming that all nucleotides have similar binding affinity toward Ac, the effective binding constant per nucleotide could be expressed as $\sqrt{3.0x10^7}$ M^{-2}, which is equal to ~$5x10^3$ M^{-1}. This value is about 5 times higher in comparison to the K_{eq} value for the Ac/HPβCD system (~$1x10^3$ M^{-1}). Though the comparison of these binding constants suggests that the dye can reside better to DNA, the observed spectral features suggest that the dye is preferentially going to the HPβCD nanocavity under the present experimental condition. The preferential binding of dye in HPβCD is understandably assisted by about five times higher concentration of HPβCD used in the solution as compared to DNA. Thus, from the experimental results, it is very evident that in the dye/HPβCD/DNA ternary system at pH 8.5, the dye can be preferentially bound to HPβCD cavity in its neutral form Ac, using a reasonably high concentration of the macrocyclic host and thereby resisting the dye binding to the DNA host.

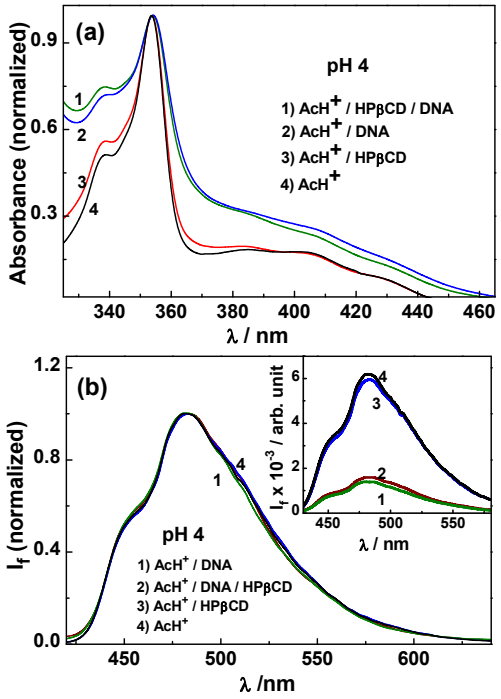

Figure 10. (a) Normalized absorption spectra for AcH^+/DNA/HPβCD, AcH^+/DNA, AcH^+/HPβCD and AcH^+ systems at pH 4. [AcH^+] = 11 μM, [HPβCD] = 10mM and DNA = 2.0 mM. **(b)** Normalized SS fluorescence spectra for AcH^+/DNA, AcH^+/DNA/HPβCD, AcH^+/HPβCD and AcH^+ systems at pH 4. [AcH^+] = 11 μM, [HPβCD] = 10mM and DNA = 2.0 mM.

Physical Chemistry Chemical Physics Accepted Manuscript

As indicated from Figure 10a & b, absorption and fluorescence spectral feature of the dye/HPβCD/DNA ternary system at pH 4 match quite well with those of the dye/DNA system, signifying that the binding feature of the dye has now just been tuned at this lower pH, for preferential binding to DNA pocket as the AcH^+ form of the dye. From the present results, it is clearly evident that HPβCD can be applied as a useful pH sensitive delivery nano-vehicle for the supply of the dye/drug to the target DNA for a programmed acidolysis. The fact that the HPβCD macrocycle shows negligible or no interaction with either the free AcH^+ or the AcH^+/DNA complex is also evidenced from the results shown in the Inset of Figure 10b where there is hardly any observable difference in the fluorescence spectra between the AcH^+ only and AcH^+/HPβCD systems and also between AcH^+/DNA and AcH^+/DNA/HPβCD systems.

1.3.2. Circular dichroism measurements: It is known that Valuable information on supramolecular host-guest complexes can be obtained from circular dichroism measurements.[51-53] In the present study, circular dichroism spectra were systematically recorded for Ac/HPβCD, Ac/DNA and Ac/HPβCD/DNA systems at pH 8.5 and are shown in Figure 11. Both HPβCD and DNA do not show any circular dichroism in the spectral region of the dye absorption. The free dye also does not show any circular dichroism in the above spectral region. For Ac/HPβCD system, however, there is a weak negative induced circular dichroism (ICD)[51-53] signal throughout the absorption band of the dye (cf. Figure 11a), certainly arises due to the axial incorporation of the dye into the HPβCD cavity.[51-53] For Ac/DNA system, there is a relatively stronger positive ICD signal throughout the absorption band of the dye (cf. Figure 11b). We attribute this strong ICD signal to the intercalation of dye into the DNA base pairs. Interestingly, for the Ac/HPβCD/DNA ternary system, the positive ICD signal (due to Ac/DNA intercalative interaction) reduces drastically and a weak negative signal develops at the lower wavelength region of the spectra (cf. Figure 11c), possibly due to the preferential formation of the Ac/HPβCD inclusion complex that displays a negative ICD signal (cf. Figure 11a). Present results thus clearly indicate that at pH 8.5 the Ac form of the dye preferentially binds to the HPβCD host, possibly through the axial incorporation of the dye into the host cavity.[51-53]

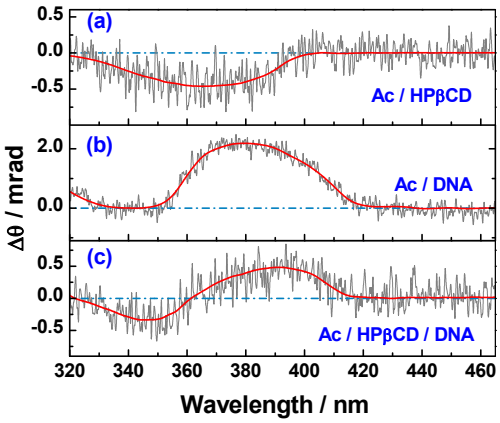

Figure 11: Circular dichroism spectra of (a) Ac/HPβCD, (b) Ac/DNA and (c) Ac/HPβCD/DNA systems (pH 8.5). Concentrations of the components were: [Ac] = 50 μM, [HPβCD] = 20 mM and [DNA] = 1.2 mM.

Circular dichroism spectra were also recorded in this study for AcH^+/HPβCD, AcH^+/DNA and AcH^+/HPβCD/DNA systems at pH 4 and the results are shown in Figure S8 of SI. As expected, the free AcH^+ did not show any circular dichroism. For the AcH^+/HPβCD system also (cf. Figure S8a), there is no observable ICD signal throughout the spectral region of the dye, suggesting no significant interaction of AcH^+ with HPβCD host. For the AcH^+/DNA system, there is a positive ICD signal (cf. Figure S8b), albeit with much weaker intensity than that of the Ac/DNA system (cf. Figure 11b), possibly suggests that at pH 4 only a small fraction of AcH^+ undergoes intercalative binding and results in the observed weak ICD signal while the majority of AcH^+ undergoes electrostatic binding to the phosphate backbone of DNA and does not contribute to the ICD signal. For the AcH^+/HPβCD/DNA ternary system, the ICD spectrum (cf. Figure S8c) is quite similar to that of the AcH^+/DNA system (cf. Figure S8b), suggesting that at pH 4 the AcH^+ form of the dye remains almost exclusively bound to DNA even in the presence of significantly high concentration of HPβCD host.

1.3.3. Time-resolved fluorescence studies: Time-resolved (TR) fluorescence is a sensitive technique to characterize multiple emissive species present in a system. TR fluorescence studies were therefore carried out on the present dye/host systems to get more insight of the complexation processes, especially the pH responsive selection of acridine dye by HPβCD or DNA hosts. Excited-state lifetimes of AcH^+ and Ac as estimated following TR fluorescence studies at pH 4 and 8.5 (decays were single exponential at both the pH conditions; cf. Figure 12a and b, respectively) are 32 ns and 9.83 ns, respectively, very similar to the values reported in the literature.[36, 37] Fluorescence decays for the dye in the presence of DNA, HPβCD and DNA/HPβCD mixture at pH 4 and 8.5 are displayed in Figure 12a & b, respectively. In these cases, the decays are either bi- or tri-exponential in nature. Different fluorescence decay parameters as obtained for these systems are listed in Table 1.

Table 1: Fluorescence decay parameters for (1) only dye, (2) dye/DNA, (3) dye/HPβCD (4) dye/HPβCD/DNA at pH 4 and 8.5. Excitation wavelength was 374 nm and emission wavelengths were 485 nm at pH 4 and 410 nm at pH 8.5 respectively.

System	pH	A_1 (%)	τ_1[a] [ns]	A_2 (%)	τ_2[a] [ns]	A_3 (%)	τ_3[a] [ns]
AcH^+	4	100	32.00				
AcH^+/DNA	4	96	29.00	4	1.52		
AcH^+/HPβCD	4	100	31.4				
AcH^+/HPβCD/DNA	4	96.5	28.9	3.5	1.6		
Ac	8.5	100	9.83				
Ac/DNA	8.5	79	8.65	21	0.48		
Ac/HPβCD	8.5	46	8.95	54	2.27		
Ac/HPβCD/DNA	8.5	34	8.6	52	2.27 (fixed)[b]	14	0.48 (fixed)[b]

[a] Error limit in the lifetime values is about 5%. **[b]** These shorter lifetime components were needed to be fixed for a consistency to the proposed model and to obtain a good fit to the observed decays.

For dye/DNA system at pH 4, the decay is biexponential in nature (cf. Figure 12b). In this case, the longer lifetime

This journal is © The Royal Society of Chemistry [year]

Physical Chemistry Chemical Physics Accepted Manuscript

component (τ_1 ~29 ns) is marginally shorter than that of the free dye (~32 ns) and is attributed to the electrostatically bound (exo- or semi-intercalative binding) AcH^+ to DNA. The shorter lifetime component (τ_2 ~1.52 ns), which is drastically shorter than that of the free dye and shows only a small contribution in the overall decay is understandably due to the fraction of the AcH^+ intercalated between DNA bases.[33, 54] The observation that the contribution of the longer lifetime component is very high (a_1 ~96%) in the present case suggests that at acidic pH the major fraction of AcH^+ undergoes exo- or semi-intercalative binding to DNA, due to strong electrostatic interaction between the cationic dye and the negative phosphate groups of the DNA backbone. Such an inference is also supported by the results obtained from circular dichroism studies, discussed in Section 1.3.2, and TR fluorescence anisotropy studies, discussed in the next section. The reduction in the fluorescence lifetime compared to that of the free dye, is regarded as due to a quenching process caused by the nucleobases, possibly through photoinduced electron transfer interaction,[33, 54-56] which is understandably very strong for the intercalated dye than the externally bound dye.

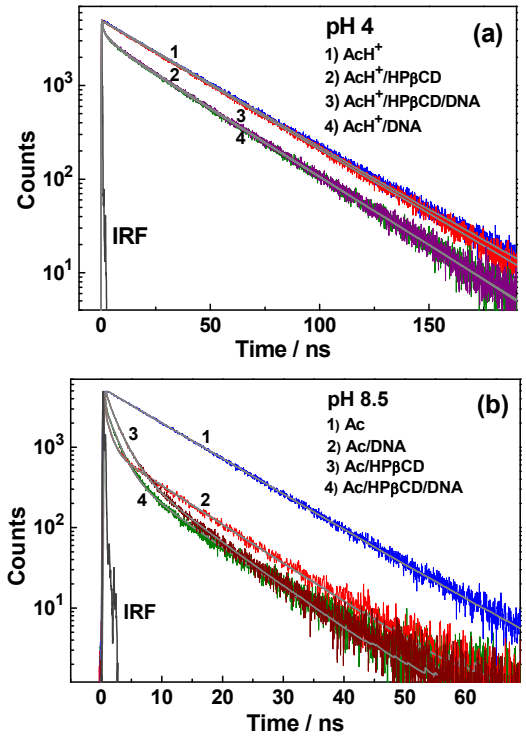

Figure 12. (a) Fluorescence decay measured at 490 nm for AcH^+, AcH^+/HPβCD, AcH^+/HPβCD/DNA and AcH^+/DNA systems at pH 4. [AcH^+] = 11 μM, [HPβCD] = 10mM and DNA = 2.0 mM. **(b)** Fluorescence decay measured at 410 nm for Ac, Ac/DNA, Ac/HPβCD and Ac/HPβCD/DNA systems at pH 8.5. [Ac] = 11 μM, [HPβCD] = 10mM and DNA = 2.0 mM. IRF represent instrument response function.

Fluorescence decay for the dye/DNA system at pH 8.5 (cf. Figure 12b) is also bi-exponential in nature, with longer lifetime component (τ_1 ~8.65 ns) marginally shorter and the shorter lifetime component (τ_2 ~0.48 ns) drastically shorter than that of the free dye (~9.83 ns). Since no appreciable electrostatic interaction is expected for the neutral Ac form of the dye with DNA, we anticipate that shorter and longer lifetime components at pH 8.5 correspond to the intercalated and the free dyes, respectively, for which supporting evidences are obtained from the fluorescence anisotropy results discussed in the next section. To be mentioned here that for both AcH^+ and Ac, the percentage reduction in the fluorescence lifetime due to DNA intercalation is very similar, about 94-95% compared to that of the free dye. Therefore, the observation that the shorter lifetime component has a relatively higher contribution at pH 8.5 (21%) than at pH 4 (4%) suggests that the intercalation of the neutral Ac form of the dye into DNA is at least five times more favoured than that of the protonated AcH^+ form of the dye.

For the dye/HPβCD system also, the fluorescence decay exhibits bi-exponential nature at pH 8.5 (cf. Figure 12b). The shorter lifetime component (τ_2 ~2.27 ns) is justifiably assigned to Ac encapsulated into HPβCD cavity where a large reduction in the fluorescence lifetime compared to that of free Ac (~9.83 ns) arises due to strong fluorescence quenching caused by the H-bonding interaction of the bound dye with the portal OH groups of the HPβCD host.[19] Longer lifetime component (τ_1 ~8.95 ns), which is just marginally shorter than that of the dye alone solution (~9.83 ns) is suggested to be due to the small fraction of the free dye that undergoes a dynamic fluorescence quenching by the HPβCD host, possibly involving the similar hydrogen bonding interaction. It should be mentioned that a similar quenching interaction for acridine dye has already been reported in our earlier study involving parent βCD host.[19]

Interestingly, the fluorescence decay for the Ac/HPβCD/DNA ternary system at pH 8.5 resembles quite closely with that of the Ac/HPβCD system but differ very largely from that of the Ac/DNA system (cf. Figure 12b). It is thus evident from the comparison of the fluorescence decays that in mildly basic solution, the Ac form to the dye in the Ac/HPβCD/DNA ternary system can be made preferentially bound to the HPβCD host, even in the presence of substantial concentration of DNA. In the present case, since multiple emissive species are present in the solution (cf. Table 1), the decay trace understandably required at least a tri-exponential function to fit acceptably and to be consistent with the proposed model, where the two shorter lifetime components correspond to the dye/DNA (τ_2 = 0.48 ns) and dye/HPβCD complexes (τ_3 = 2.27 ns) and the longer lifetime component (τ_1 = 8.6 ns) represents the fraction of the free dye that undergo dynamic quenching jointly by HPβCD and DNA hosts present in the solution.

Fluorescence decays for the dye at different dye/host combinations at pH 4 are shown in Figure 12a. As already mentioned, at pH 4 the fluorescence decay of the dye in the absence of any host is single exponential in nature with lifetime about 32 ns. For the dye/HPβCD system at pH 4, the decay interestingly shows a single exponential nature, with only a small but quite systematic reduction in the lifetime with the HPβCD concentration. This observation suggests that AcH^+ form does not undergo any appreciable inclusion complex formation but the free excited dye undergoes a small extent of dynamic quenching by the HPβCD host. An important observation to be noted from Figure 12a is that the decay for the AcH^+/DNA/HPβCD ternary system exactly superimposes with that of the AcH^+/DNA system, confirming that at acidic pH the dye is completely bound to the DNA host as its AcH^+ form. Observed TR fluorescence results are thus in complete correspondence with the results obtained

Physical Chemistry Chemical Physics Accepted Manuscript

from ground state absorption and SS fluorescence studies, clearly indicating that in the dye/HPβCD/DNA ternary system the HPβCD in effect act as a receptor to bind and stabilize the dye at higher pH and renders complete relocation of the dye to the desired DNA target just on reducing the pH of the solution to the acidic region. In other words, HPβCD acts as an efficient nano-transporter to carry the dye/drug to the target DNA and delivers the model drug to the target on using the pH drop as the stimulus.

1.3.4. Fluorescence anisotropy studies: Fluorescence anisotropy decays for acridine dye were measured at pH 4 and 8.5, both in the absence and in presence of DNA, HPβCD and DNA/HPβCD mixture. Observed anisotropy decays for different systems at pH 4 and 8.5 are presented in Figure 13a & b, respectively. Analysis of these decays required either mono-exponential or bi-exponential functions, to obtain satisfactory fits. The anisotropy decay parameters obtained for the dye in different experimental conditions are listed in Table 2.

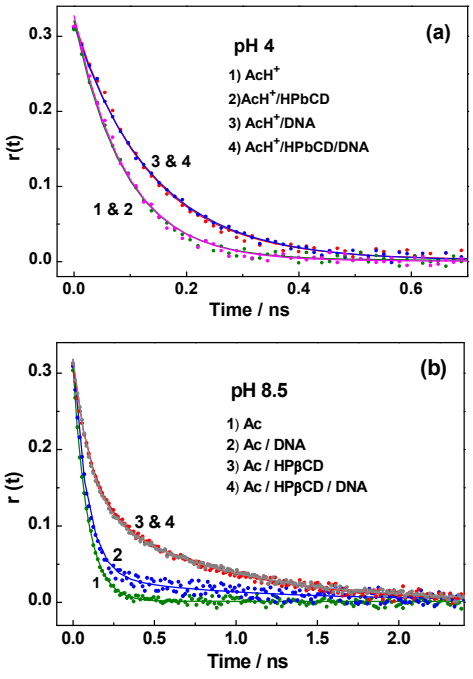

Figure 13. (a) Time-resolved anisotropy decay curves for AcH^+, AcH^+/HPβCD, AcH^+/HPβCD/DNA and AcH^+/DNA systems at pH 4. **(b)** Time-resolved anisotropy decay curves for Ac, Ac/DNA, Ac/HPβCD and Ac/HPβCD/DNA systems at pH 8.5.

As expected, the anisotropy decays for the free dye are very fast and follow mono-exponential kinetics both at pH 4 and 8.5, giving the rotational time constants (τ_{r1}) as about ~90 ps for both AcH^+ (pH 4) and Ac (pH 8.5) forms of the dye. At pH 4, the decay for AcH^+/HPβCD system also follows a mono-exponential kinetics and gives the τ_{r1} value (~90 ps) very similar to that of the free AcH^+. It is thus evident that there is no appreciable interaction of AcH^+ with HPβCD host, as also inferred from SS and TR fluorescence and circular dichroism results. Contrary to the AcH^+/HPβCD system, for the AcH^+/DNA system at pH 4, the anisotropy decay is relatively slower and fits well with a mono-exponential function giving a τ_{r1} value (~140 ps) significantly higher than that of the free dye, although the increase is not exceedingly large. Recalling TR fluorescence results in Table 1, it was indicated that in AcH^+/DNA system at pH 4 there is a longer lifetime component τ_1 that shows the largest contribution (~96%) and was attributed to exo-bound AcH^+ with DNA, while the shorter lifetime component τ_2, showing only a small contribution (~4%), was ascribed to the intercalatively bound AcH^+ to DNA. In accordance with these TR fluorescence results, it is expected that the anisotropy decay for the AcH^+/DNA system at pH 4 will be mainly due to the exo-bound AcH^+ and hence should effectively follow a mono-exponential function.[57] Since the exo-bound AcH^+ with DNA is expected to suffer only a small retardation in its rotational motion, the τ_{r1} value for the present system is accordingly increased only to a small extent as compared to that of the free dye.

Table 2: Fluorescence anisotropy decay parameters for (1) dye only, (2) dye/DNA, (3) dye/HPβCD (4) dye/HPβCD/DNA at pH 4 and 8.5. Excitation wavelength was 374 nm and emission wavelengths were 485 nm at pH 4 and 410 nm at pH 8.5 respectively.

System	pH	$r_{1,0}$	τ_{r1}[a] [ps]	$r_{1,0}$	τ_{r2}[a] [ps]
AcH^+	4	0.32	90		
AcH^+/HPβCD	4	0.32	91		
AcH^+/DNA	4	0.31	138		
AcH^+/HPβCD/DNA	4	0.32	133		
Ac	8.5	0.31	89		
Ac/HPβCD	8.5	0.17	95	0.14	760
Ac/DNA	8.5	0.28	89	0.03	910
Ac/HPβCD/DNA	8.5	0.18	96	0.14	770

[a] Error limit in the lifetime values is about 5%.

At pH 8.5, for both Ac/HPβCD and Ac/DNA systems, the anisotropy decays follow bi-exponential kinetics. In both the cases, the τ_{r1} component is very similar to that of the free dye while the τ_{r2} component is drastically higher in comparison to τ_{r1}. As observed in the TR fluorescence studies (cf. Table 1), for the present systems, the fluorescence decays are dominated by a longer lifetime component τ_1 attributed to the fraction of the free dye present in the solution. The observation that τ_{r1} component for both Ac/HPβCD and Ac/DNA systems resembles that of the free dye thus directly supports the proposition made from the TR fluorescence results. That the τ_{r2} component for both dye/HPβCD and dye/DNA systems is much higher than τ_{r1} clearly suggests that this component is due to the Ac bound to the respective hosts, via inclusion complex formation with HPβCD cavity and through intercalative bounding to DNA host. This is further supported by the fact that the τ_{r2} value for the Ac/DNA system is much higher than that of the Ac/HPβCD system, understandably because the rotational motion of the intercalatively bound dye to DNA will be much more restricted in comparison to that of the dye incorporated into the HPβCD cavity. Further, from the comparison of the τ_{r2} value (910 ps) in Ac/DNA system at pH 8.5 with the τ_{r1} value (140 ps) in AcH^+/DNA system at pH 4 it is evident that the rotational motion of the DNA-bound Ac form is much more retarded than the DNA bound AcH^+ form of the dye. This is in direct support of our inference that in AcH^+/DNA system at pH 4, the cationic AcH^+ form of the dye mainly undergoes an exo-binding to DNA through electrostatic interaction whereas in Ac/DNA system at pH 8.5 the neutral Ac form of the dye mainly undergoes the intercalative mode of

This journal is © The Royal Society of Chemistry [year]

Physical Chemistry Chemical Physics Accepted Manuscript

binding with the DNA host. For dye/HPβCD system at pH 8.5, the longer τ_{r2} component is certainly due to the inclusion of Ac into HPβCD cavity which causes a large increase in the hydrodynamic volume of the fluorophore and hence an increase in the rotational time constant.

For the Ac/HPβCD/DNA ternary system at pH 8.5, the estimated anisotropy decay parameters (cf. Table 2 and Figure 13b), match quite closely with those obtained for the Ac/HPβCD system. These results strongly supports our proposition that in Ac/HPβCD/DNA ternary system at pH 8.5 a major fraction of Ac actually remained bound to the HPβCD cavity, even in the presence of the significantly high concentration of DNA. On the contrary, at acidic pH, the anisotropy decay for the AcH^+/HPβCD/DNA ternary system, interestingly resembles quite closely to that of the AcH^+/DNA system (cf. Figure 13a and Table 2). This observation directly reinstates the fact that at acidic pH the AcH^+ form of the dye almost exclusively binds to the DNA host, even in the presence of substantially high HPβCD concentration. Thus, the observed results in effect suggest that depending upon the pH of the solution, the HPβCD host not only selectively binds but also releases the active dye to the target DNA site, induced by a suitable pH change.

In brief, fluorescence anisotropy results correspond very nicely with the ground state absorption and the SS and TR fluorescence results and establish the fact that the reduction in the pH of the solution can provide a simple stimulus to quantitatively release the dye from the HPβCD cavity for its binding to the target DNA in a dye/HPβCD/DNA ternary system. Such a strategy of controlled dye/drug release mechanism can be easily visualized by the schematic presentation shown in Scheme 3. From the present model study it is evident that HPβCD nanocarrier can effectively be used for controlled and targeted release of potential anticancer prodrug under acidic condition and thereby to selectively increase the local drug concentration at the targeted site, reducing the untoward side effect of the drug, an advantage that is highly desired in chemotherapeutic applications.

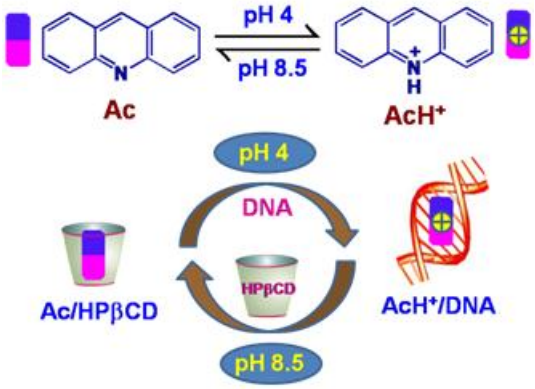

Scheme 3: Schematic representation of the pH-induced transfer of acridine from HPβCD to DNA at acidic pH and vice versa.

Conclusions

Interaction of an anticancer active acridine dye with HPβCD, DNA, HPβCD/DNA mixture has been investigated, using ground state absorption, steady-state fluorescence, time-resolved fluorescence, fluorescence anisotropy decay, ^{1}H NMR and circular dichroism measurements at different pH conditions. Results show that HPβCD selectively and strongly encapsulates the neutral dye Ac but shows almost no affinity for the protonated dye AcH^+. On the contrary, DNA interacts strongly with both AcH^+ and Ac forms of the dye, albeit with somewhat higher affinity for the Ac form. Consequently, the differential binding of the two prototropic forms of acridine dye observed with HPβCD and DNA hosts leads to about 1.0 unit of downwards pK_a shift for the dye/HPβCD system and about 0.4 unit of downwards pK_a shift for the dye/DNA system. Using acridine dye/HPβCD/DNA ternary system as a model, we demonstrate in this study the interesting strategy of pH dependent formation and dissociation of the dye/HPβCD complex, for a targeted and controlled release of the dye from biocompatible model drug carrier HPβCD nanocavity to the target DNA site. In the dye/HPβCD/DNA ternary supramolecular system, HPβCD not only selectively binds and stabilizes the neutral Ac form of the dye at the mildly alkaline pH but also explicitly delivers the active protonated AcH^+ form of the dye to the target DNA, triggered by a decrease in the pH to mildly acidic condition. Thus, HPβCD acts as a model drug delivery agent to carry the dye to the target acceptor DNA. Potentiality of this unique supramolecular assembly may be explored in real biological systems where acidolysis can be used as a trigger for the controlled dissociation of the prodrug from the HPβCD inclusion complexes, leading to the association of the active form of the drug to the target site, such as to tumour cells or at the acidic organelles region, making the dye/drug to be more effective for the desired activity, with maximum selectivity. This model study would be very beneficial in relation to chemotherapeutic applications, nano reactors, pharmaceutical development and also can be useful in designing new and promising stimuli-responsive assemblies for different biomedical applications. Future studies aim at to investigate more on the interaction of anticancer acridine drugs with potential cyclodextrin derivatives for real pH responsive biomedical applications.

Experimental Section

Acridine dye (purity >99%) was obtained from Sigma–Aldrich, USA, and purified by re-crystallization from cyclohexane solution. Hydroxypropyl-β-cyclodextrin (HPβCD, *cf.* Scheme 1; average degree of substitution = 0.8, average MW = 1500) was purchased from Aldrich and used as received. Calf thymus DNA (ct DNA) was purchased from Sigma and used as received. Nanopure water (Barnstead System; conductivity of 0.1 μS cm^{-1}) was used for all solution preparations. Dye solution was prepared by directly dissolving the dye sample and estimating its concentration from the absorption spectral measurement (extinction coefficient 17,793 $M^{-1}cm^{-1}$ at λ_{max} 355 nm for AcH^+ and 9,700 $M^{-1}cm^{-1}$ at λ_{max} 355 nm for Ac).[19] Known weight of HPβCD was directly added to the experimental solution to achieve the required host concentration. Stock *ct*-DNA solution was prepared by dissolving the solid DNA sample in nanopure water and keeping the solution stored overnight at 4 °C. Each time fresh DNA solution was prepared to perform the experiments. As *ct*-DNA has quite a large distribution in the molecular sizes (8.0-15 kb), the concentration of DNA in the experimental solution was determined in terms of total nucleotide

Physical Chemistry Chemical Physics Accepted Manuscript

concentration, following absorbance at 260 nm and using an extinction coefficient of 6600 $M^{-1}cm^{-1}$.[58-60] That the DNA sample is free from protein impurities was ensured by observing the ratio of absorbance at 260 nm to that at 280 nm in the range of 1.8-1.9.[58-60]

All the measurements were carried out in aqueous solutions at suitable pH conditions at ambient temperature (~25 ^{o}C). The pH of the solutions was adjusted by adding dilute perchloric acid or dilute sodium hydroxide in small steps and the pH was measured by using a pH meter (CL/46, Toshcon make, India). Ground state absorption spectra and steady-state fluorescence spectra were recorded using a Jasco UV-visible spectrophotometer (model V-650; Tokyo, Japan) and a Hitachi spectrofluorimeter (model F-4500; Tokyo, Japan), respectively. Time-resolved fluorescence measurements were carried out using a time-correlated single-photon-counting (TCSPC) spectrometer,[57, 61] obtained from IBH, UK. In these measurements, a 374 nm diode laser (pulse width ~ 100 ps, repetition rate 1 MHz) was used as the excitation source and a special photomultiplier tube (PMT)-based detection module supplied by Horiba Jobin Yvon IBH was used for the fluorescence detection. Instrument response function (IRF) for the TCSPC setup was measured by using scattered light from TiO_2 suspension in water and the full width half maximum (FWHM) of the IRF was found to be ~120 ps. All the measurements were carried out at magic angle configuration to eliminate the effect of rotational anisotropy on the observed fluorescence decays. Observed decays were in general analyzed as a sum of exponentials (cf. eq. 2), following a reconvolution procedure.[57, 61]

$$I(t) = \sum B_i \exp(-t / \tau_i) \quad (2)$$

where B_i and τ_i are the pre-exponential factor and fluorescence lifetime, respectively, for the i^{th} decay component. The quality of the fits and consequently the exponentiality of the decays were judged from the reduced chi-square (χ^2) values and the distribution of the weighted residuals among the data channels.[57, 61] For time resolved fluorescence anisotropy measurements, the fluorescence decays, $I_{||}(t)$ and $I_{\perp}(t)$, corresponding to the parallel and perpendicular emission polarizations, respectively, with respect to the vertically polarized excitation light, were first measured. These decays were used to construct the anisotropy decay function r(t) as,[57, 61]

$$r(t) = \frac{I_{||}(t) - GI_{\perp}(t)}{I_{||}(t) + 2GI_{\perp}(t)} \quad (3)$$

where G is the correction factor for the polarization bias of the detection setup. Value of G was obtained independently by measuring two perpendicularly polarized fluorescence decays while the sample was excited with the horizontally polarized excitation light.[57, 61] The ^{1}H NMR measurements were carried out using a Bruker 600 MHz NMR spectrometer. In the present measurements, the required solutions (~150 μM of dye and HPβCD each and 300 μM of DNA) were prepared in D_2O (99.8%) solvent. Required pD of the solutions were adjusted by adding dilute NaOD and DCl solutions in small steps and measured by using the pH meter. The circular dichroism spectra were recorded using a UV-vis spectrophotometer/polarimeter model MOS-450 from Biologic Science Instruments, France.

Acknowledgement

Authors are thankful to Dr. A. Barik of RPCD and Dr. S. Dey of Chemistry Division, BARC, for their help in the circular dichroism and NMR measurements, respectively. Authors also thankfully acknowledge the Bhabha Atomic Research Centre, Mumbai, India, for the generous support provided during the course of the present research work.

Notes and references

[a] *Radiation & Photochemistry Division, Bhabha Atomic Research Centre, Trombay, Mumbai 400 085, INDIA Fax: (+) 91-22-25505151, E-mail: msayed@barc.gov.in, hpal@barc.gov.in*

† Electronic Supplementary Information (ESI) available: [details of any supplementary information available should be included here]. See DOI: 10.1039/b000000x/

1. R. L. Carrier, L. A. Miller and I. Ahmed, *J Control Release* 2007, **123**, 78-99.
2. K. Uekama, F. Hirayama and T. Irie, *Chem. Rev.*, 1998, **98**, 2045-2076.
3. D. W. Kuykendall and S. C. Zimmerman, *Nat. Nanotechnol.*, 2007, **2**, 201–202.
4. G. Astray, C. Gonzalez-Barreiro, J. C. Mejuto, R. Rial-Otero and J. Simal-Gandara, *Food Hydrocolloid*, 2009, **23**, 1631–1640.
5. Z. Qi and C. A. Schalley, *Acc. Chem. Res.*, 2014, 47, 2222−2233.
6. M. D. Pluth, R. G. Bergman and K. N. Raymond, *Science* 2007, **316**, 85–88.
7. E. M. M. D. Valle, *Process Biochem.*, 2004, 39, 1033–1046
8. K. Langa, J. Mosinger and D. M. Wagnerová, *Coordin. Chem. Rev.* , 2004, **248**, 321–350.
9. H. Yamaguchi, T. Ogoshi and A. Harada, John Wiley & Sons, New Jersey, 2011.
10. M. Shaikh, S. D. Choudhury, J. Mohanty, A. C. Bhasikuttan, W. M. Nau and H. Pal, *Chem. Eur. J.* , 2009, **15**, 12362 – 12370.
11. M. Shaikh, J. Mohanty, A. C. Bhasikuttan, V. D. Uzunova, W. M. Nau and H. Pal, *Chem. Commun.*, 2008, 3681–3683.
12. G. Chen and M. Jiang, *Chem. Soc. Rev.*, 2011, **40**, 2254–2266.
13. J. Zhang and P. X. Ma, *Adv. Drug Deliver. Rev.*, 2013, **65**, 1215–1233.
14. I. Ghosh and W. M. Nau, *Adv. Drug Deliver. Rev.*, 2012, **64**, 764–783.
15. Y. Cao, X. Hu, Y. Li, X. Zou, S. Xiong, C. Lin, Y. Shen and L. Wang, *J. Am. Chem. Soc.*, 2014, **136**, 10762−10769.
16. V. T. Perchyonok and T. Oberholzer, *Curr. Org. Chem.*, 2012, **16**, 2365-2378.
17. T. Loftsson and D. Duchene, *Int. J. Pharm.*, 2007, **329**, 1–11.
18. W. Al-Soufi, B. Reija, M. Novo, S. Felekyan, R. Kuhnemuth and C. A. M. Seidel, *J. Am. Chem. Soc.*, 2005, **127**, 8775-8784.
19. M. Shaikh, Y. M. Swamy and H. Pal, *J. Photochem. Photobiol. A* 2013, **258**, 41– 50.
20. M. Shaikh, J. Mohanty, P. K. Singh, W. M. Nau and H. Pal, *Photochem. Photobiol. Sci.* , 2008, **7**, 408-414.
21. V. Khorwal, B. Sadhu, A. Dey, M. Sundararajan and A. Datta, *J. Phys. Chem. B*, 2013, **117**, 8603–8610.
22. S. Gould and R. C. Scott, *Food Chem. Toxicol.*, 2005, **43**, 1451–1459.

This journal is © The Royal Society of Chemistry [year]

Physical Chemistry Chemical Physics Accepted Manuscript

23. Z. Huang, S. Tian, X. Ge, J. Zhang, S. Li, M. Li, J. Cheng and H. Zheng, *Carbohyd. Polym.*, 2014, **107**, 241–246.
24. K. Miyake, H. Arima, F. Hirayama, M. Yamamoto, T. Horikawa, H. Sumiyoshi, S. Noda and K. Uekama, *Pharm. Dev. Technol*, 2000, **5**, 399–407.
25. C. Liu, Z. Jiang, Y. Zhang, Z. Wang, X. Zhang, F. Feng and S. Wang, *Langmuir*, 2007, **23**, 9140-9142.
26. A. Rescifina, C. Zagni, M. G. Varrica, V. Pistarà and A. Corsaro, *Eur. J. Med. Chem.*, 2014, **74**, 95-115.
27. S. Monti and I. Manet, *Chem. Soc. Rev.*, 2014, **43**, 4051--4067.
28. X. Chen, L. Chen, X. Yao, Z. Zhang, C. He, J. Zhang and X. Chen, *Chem. Commun.*, 2014, **50**, 3789—3791.
29. A. Rajendran and B. U. Nair, *Biochim. Biophys. Acta* 2006, **1760**, 1794–1801.
30. P. Belmont, J. Bosson, T. Godet and M. Tiano, *Anti-Cancer Agent Me.*, 2007, **7**, 139-169.
31. A. J. Pickard, F. Liu, T. F. Bartenstein, L. G. Haines, K. E. Levine, G. L. Kucera and U. Bierbach, *Chem. Eur. J.* , 2014, **20**, 1 – 15.
32. F. Charmantray, M. Demeunynck, D. Carrez, A. Croisy, A. Lansiaux, C. Bailly and P. Colson, *J. Med. Chem.* , 2003, **46**, 967-977.
33. K. Kawai, Y. Osakada, M. Fujitsuka and T. Majima, *J. Phys. Chem. B*, 2008, **112**, 2144-2149.
34. H. W. Zimmermann, *Angew. Chem. Int. Ed. Engl.* , 1986, **25**, 115-130.
35. R. W. Armstrongy, T. Kurucsev and U. P. Strauss, *J. Am. Chem. Soc.*, 1970, **92**, 3174-3180.
36. M. K. Sarangi and S. Basu, *Phys. Chem. Chem. Phys.*, 2011, **13**, 16821-16830.
37. V. Kumar, A. Pandey and S. Pandey, *ChemPhysChem*, 2013, **14**, 3944 – 3952.
38. R. Wang, L. Yuan, H. Ihmels and D. H. Macartney, *Chem. Eur. J.* , 2007, **13**, 6468–6473.
39. M. S. Ibrahim, I. S. Shehatta and A. A. Al-Nayeli, *J. Pharm. Biomed. Anal.* , 2002, **28**, 217–225.
40. G. Zhang, Y. Pang, S. Shuang, C. Dong, M. M. F. Choi and D. Liu, *J. Photochem. Photobiol. A*, 2005, **169**, 153–158.
41. G. Zhang, X. Hu, N. Zhao, W. Li and L. He, *Pestic. Biochem. Phys.*, 2010, **98**, 206–212.
42. C. Y. Huang, *Method. Enzymol.* , 1982, **87**, 509–525.
43. M. Sayed, F. Biedermann, V. D. Uzunova, K. I. Assaf, A. C. Bhasikuttan, H. Pal, W. M. Nau and J. Mohanty, *Chem. Eur. J.*, 2015, **21**, 691– 696.
44. J. M. Schuette, T. T. Ndou, A. M. d. l. Pela, S. Mukundan and I. M. Warner, *J. Am. Chem. SOC.*, 1993, **115**, 292-298.
45. J. Carlstedt, A. González-Pérez, M. Alatorre-Meda, R. S. Dias and B. Lindman, *Int. J. Biol. Macromol.*, 2010, **46**, 153–158.
46. Y. Huang, Q. Lu, J. Zhang, Z. Zhang, Y. Zhang, S. Chen, K. Li, X. Tan, H. Lin and X. Yua, *Bioorg. Med. Chem.*, 2008, **16**, 1103–1110.
47. M. Ageno, E. Dore and C. Frontali, *Biophys. J* . 1969, **9**, 1281-1311.
48. O'Connor, S. Mansy, M. Bina, D. R. McMillin, M. A. Bruck and R.S.Tobias, *Biophys. Chem.*, 1981, **15**, 53-64.
49. C. M. Muntean, G. J. Puppels, J. Greve, G. M. J. Segers-Nolten and S. Cinta-Pinzaru, *J. Raman Spectrosc.* , 2002, **33**, 784–788.
50. F. Zsila, Z. Bikádi and M. Simonyi, *Org. Biomol. Chem.* , 2004, **2**, 2902 – 2910.
51. F. Mendicuti and M. J. González-Álvarez, *J. Chem. Educ.*, 2010, **87**, 965-968.
52. M. Shaikh, J. Mohanty, M. Sundararajan, A. C. Bhasikuttan and H. Pal, *J. Phys. Chem. B*, 2012, **116**, 12450−12459.
53. Q. Wang, H. R, X. Cheng and C. Lu, *J. Incl. Phenom. Macrocycl. Chem.*, 2011, **69**, 231–243.
54. K. Fukui, K. Tanaka, M. Fujitsuka, A. Watanabe and O. Ito, *J. Photochem. Photobiol. B: Biol.*, 1999, **50**, 18-27.
55. K. Fukui and K. Tanaka, *Angew. Chem. Int. Ed.* , 1998, **37**, 158-161.
56. J. Joseph, N. V. Eldho and D. Ramaiah, *Chem. Eur. J.*, 2003, **9**, 5926 -5935.
57. J. R. Lakowicz, *Principle of fluorescence spectroscopy*, Plenum press: Springer, New York, 2006.
58. H. Joshi, A. Sengupta, K. Gavvala and P. Hazra, *RSC Adv.*, 2014, **4**, 1015–1024.
59. N. Nikolis, C. Methenitis and G. Pneumatikakis, *J. Inorg. Biochem.*, 2003, **95**, 177–193.
60. P. K. Singh and S. Nath, *J. Phys. Chem. B*, 2013, **117**, 10370−10375.
61. D. V. O'Connor and D. Phillips, Academic Press, New York, 1984.

Physical Chemistry Chemical Physics Accepted Manuscript